Supporting Information

Levin et al. 10.1073/pnas.1207362109

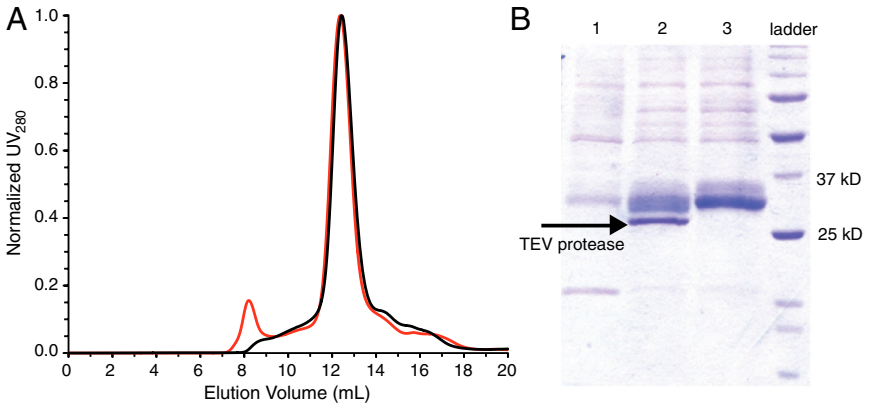

Fig. S1. *Purification of human UT-B.* (*A*) Size exclusion FPLC chromatogram showing normalized absorbance at 280 nm from bovine (black) and human (red) UT-B solubilized in DM. (*B*) SDS-PAGE gel of fractions eluted from an IMAC column after addition of 20 mM imidazole (Lane 1) or 300 mM imidazole after (Lane 2) or before (Lane 3) cleavage with TEV protease.

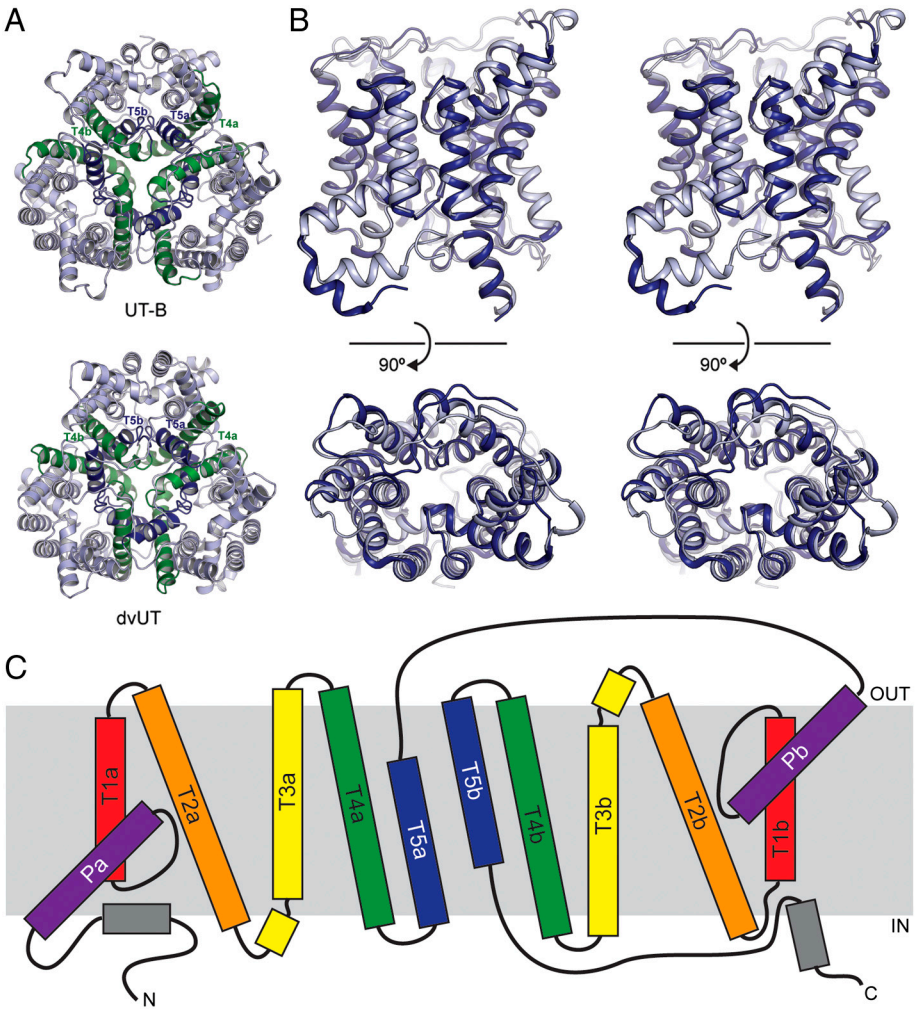

Fig. S2. *Topology and structure of the urea transporter fold.* (*A*) The bovine UT-B (*Top*) and dvUT (*Bottom*) trimers are shown with helices involved in the trimer interface highlighted. (*B*) Steoroviews of a protomer of UT-B (light blue) aligned with a protomer of dvUT (dark blue), as viewed from within the plane of the membrane (*Top*) and from the extracellular side (*Bottom*). (*C*) Diagram of the shared membrane topology of dvUT and UT-B, oriented with the intracellular side on bottom. Pairs of pseudo-symmetric, equivalent helices between the two homologous repeats are shown with the same color; dark gray helices are not involved in the homologous repeats.

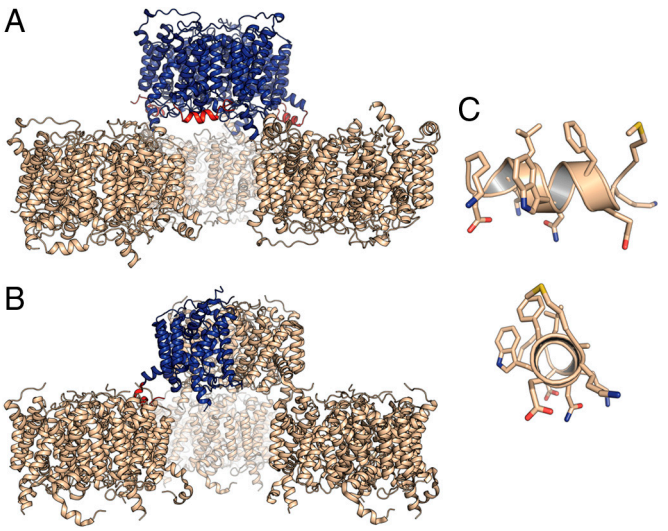

Fig. S3. *Crystal packing in urea transporter structures.* Crystal packing in the UT-B (*A*) and dvUT structures (*B*). The asymmetric units are shown in blue, and the short N-terminal helix is highlighted in red. (*C*) Side chains on the short N-terminal helix of UT-B are shown from two angles, both oriented with the membrane-facing side on top.

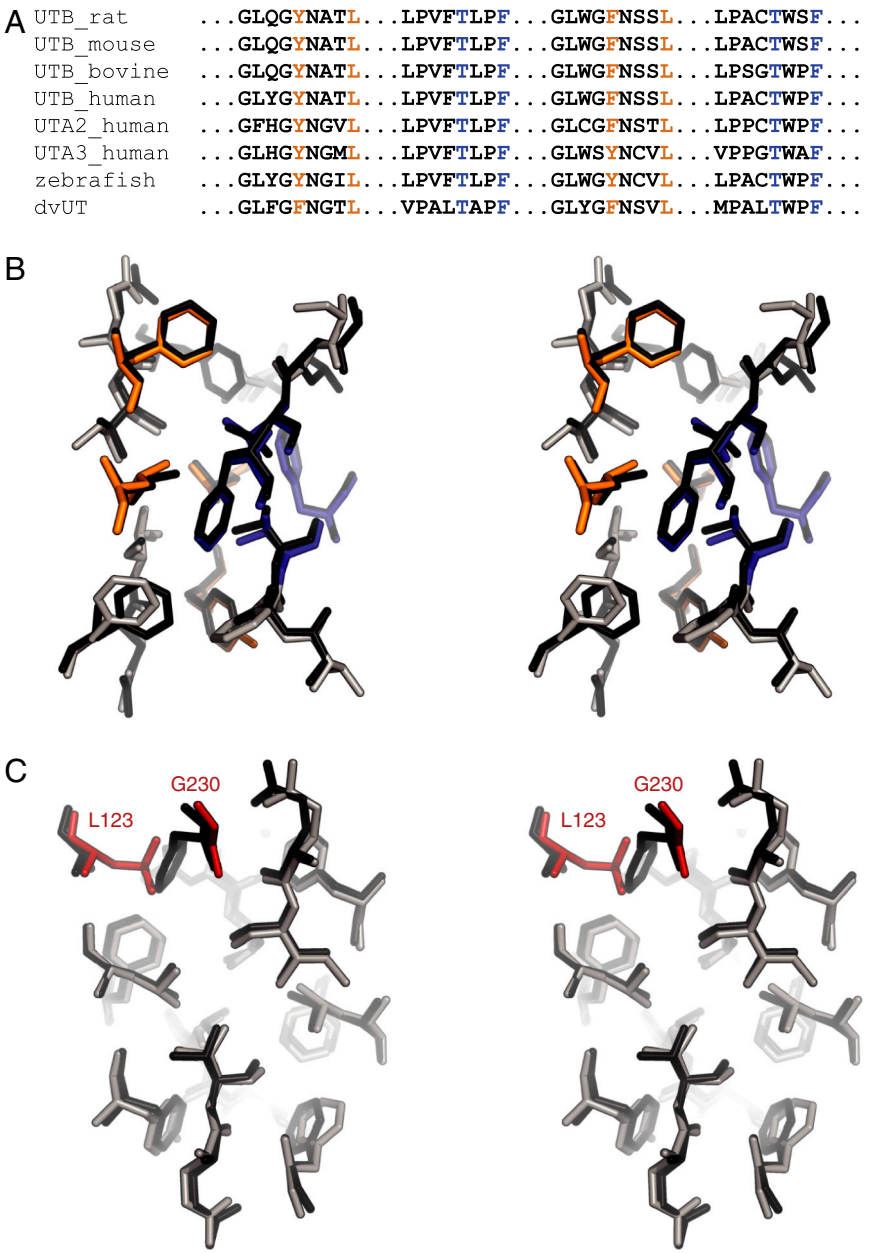

Fig. S4. *Conservation of the urea transporter pore.* (*A*) Alignment of the signature sequences from various mammalian, fish, and bacterial UTs. (*B*) Stereo view of residues in the selectivity filter of bovine UT-B (grey) aligned with dvUT (black). Residues in UT-B from the conserved signature sequences are colored according to the scheme in (*A*). (*C*) Stereo view rotated 90° around the pore axis relative to (*B*), with residues differing between the bacterial and mammalian structures marked in red. Residue numbers correspond to the mammalian sequence.

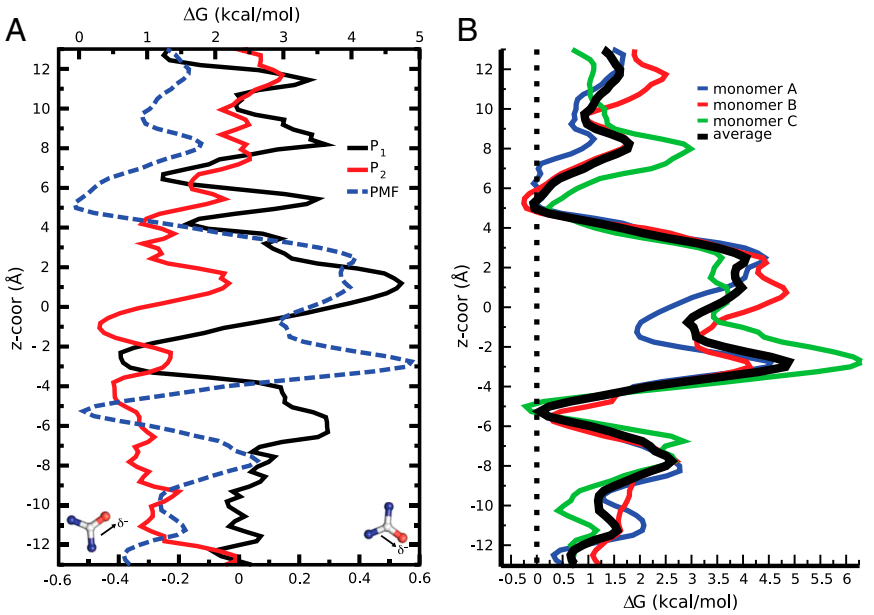

Fig. S5. *Substrate orientation and potential of mean force for urea permeation through UT-B.* (*A*) Orientational order parameters (P_1 and P_2) of urea as a function of channel axis overlaid with the PMF calculated for urea permeation through UT-B. The polar order parameter, $P_1 = \langle \hat{d} \cdot \hat{z} \rangle$, where $\hat{d}$ and $\hat{z}$ are the unit vectors of the dipole moment of urea and the channel axis, respectively, captures the orientation of urea with respect to the channel axis; the images of urea molecules along the *Bottom* of the figure indicate the direction of negative vs. positive values when the pore is oriented with the extracellular side on the *Top*. The nematic order parameter, $P_2 = \frac{3\langle(\hat{d}\cdot\hat{z})^2\rangle - 1}{2}$, is used to distinguish between isotropic and ordered states. (*B*) The PMF as a function of the channel axis for the three individual subunits in UT-B (red, blue and green) and the average over all three subunits (black).

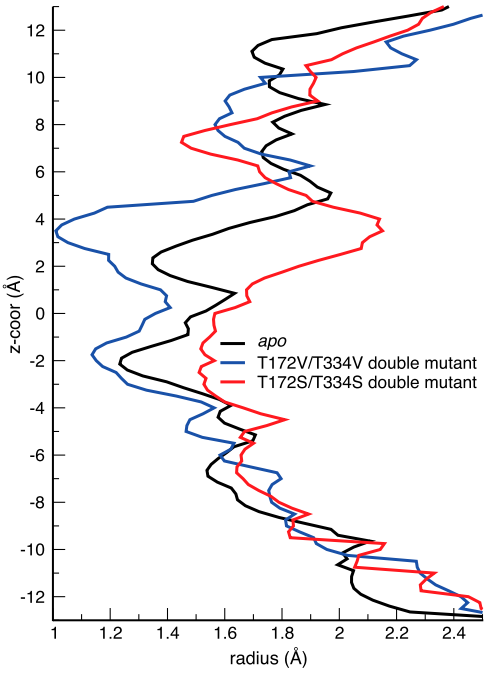

Fig. S6. *Radius of the UT-B pore.* Radius of the pore along the channel axis in WT (black), T172V/T334V (blue), and T172S/T334S (red) bovine UT-B in the equilibrium simulations, calculated by the program HOLE.

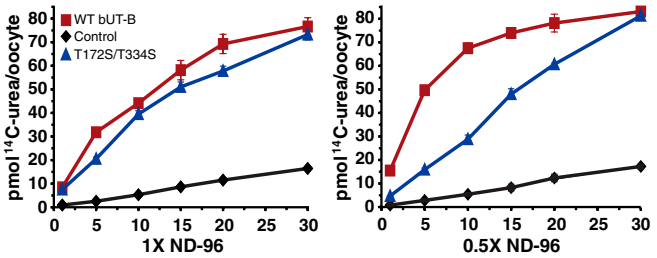

Fig. S7. *Time courses of urea uptake into oocytes in isoosmotic and hypoosmotic buffers.* ^{14}C-labelled urea uptake in WT or T172S/T334S UT-B mRNA-injected oocytes or in control oocytes over a period of 30 min, while bathed in either ND-96 buffer (*Left*) or ND-96 diluted 1:1 with distilled water (*Right*).

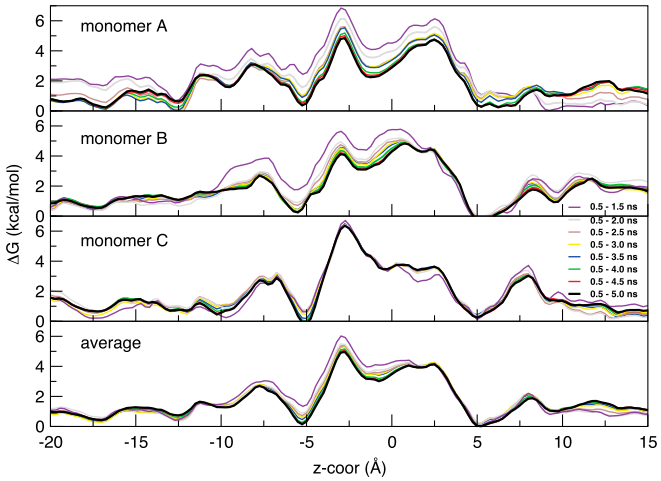

Fig. S8. *Convergence of potential of mean force.* PMFs for urea permeation calculated using sequentially increasing intervals from the umbrella sampling simulations. The changes in the PMFs are minimal after approximately 3 ns, indicating convergence of the simulations.

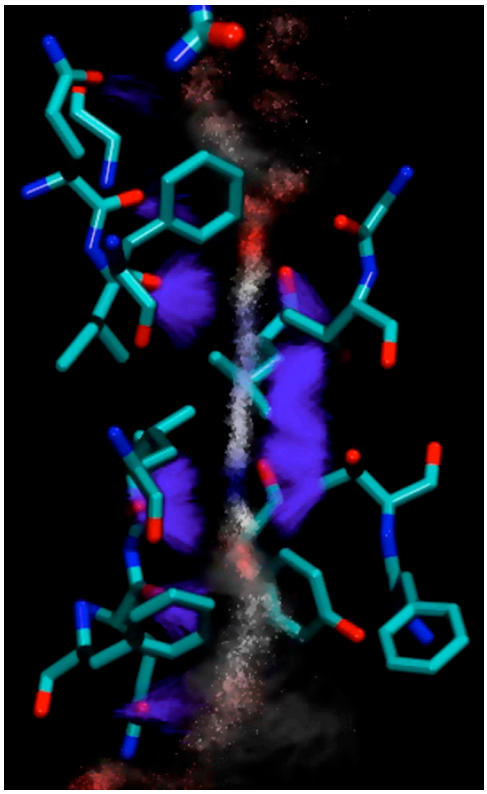

Movie S1. *Urea permeation through UT-B.* Translocation pathway and mechanism of urea permeation through monomeric UT-B as described by the molecular dynamics simulations. The trajectories of neighboring umbrella sampling windows were combined such that subsequent frames used for generating the animation are not separated by more than 1.5 Å with regard to the RMSD of urea heavy atoms. The S_i, S_m, and S_o regions and urea are shown in licorice. The dots represent all positions sampled by urea in the umbrella sampling trajectories and are colored based on PMF values of that region (low ΔG to high ΔG: red to white to blue). Purple lines indicate the hydrogen bonds between urea and the oxygen ladders as well as T172 and T334.
Movie S1 (MOV)

Table S1. Data collection, phasing, and refinement statistics

	UT-B	Se-urea UT-B
Data collection		
Space group	$P2_1$	$P2_1$
Cell dimensions		
a, b, c (Å)	74.70, 105.87, 105.87	75.00, 106.23, 105.82
β (°)	99.00	98.18
Resolution (Å)	2.35 (2.35–2.39)	2.5 (2.5–2.54)
R_{merge}	0.092 (0.585)	0.168 (0.921)
$I/\sigma(I)$	11.7 (1.51)	11.2 (1.82)
Completeness (%)	97.7 (93.4)	99.9 (100)
Redundancy	1.9 (1.7)	7.0 (6.7)
Refinement		
Resolution (Å)	2.36 (2.36–2.42)	2.5 (2.5–2.56)
No. reflections	63237 (4152)	54007 (3862)
Completeness (%)	98.9 (89.8)	99.8 (99.7)
R_{work}/R_{free} (%)	19.6 (25.3)/22.8 (28.2)	19.7 (24.4)/22.9 (27.7)
B-factors		
Protein	59.1	50.4
Ligand/ion	89.2	75.0
Water	53.2	44.0
RMS deviations		
Bond lengths (Å)	0.011	0.007
Bond angles (°)	1.42	1.19

Highest resolution shell is shown in parenthesis.